ISSN 0021-3640, JETP Letters, 2024, Vol. 120, No. 7, pp. 477–482. © Pleiades Publishing, Ltd., 2024.
Russian Text © The Author(s), 2024, published in Pis'ma v Zhurnal Eksperimental'noi i Teoreticheskoi Fiziki, 2024, Vol. 120, No. 7, pp. 498–504.

OPTICS
AND LASER PHYSICS

Ramsey Spectroscopy of CPT Resonances on the D_1 Line of Alkali Metal Atoms in Miniature Cells in the Field of Counterpropagating Waves with Opposite Circular Polarizations

V. I. Yudin[a,b,c,*], M. Yu. Basalaev[a,b,c], D. A. Radnatarov[a], I. V. Gromov[a], M. D. Radchenko[a,c], S. M. Kobtsev[a], and A. V. Taichenachev[a,b]

[a] *Novosibirsk State University, Novosibirsk, 630090 Russia*
[b] *Institute of Laser Physics, Siberian Branch, Russian Academy of Science, Novosibirsk, 630090 Russia*
[c] *Novosibirsk State Technical University, Novosibirsk, 630073 Russia*
**e-mail: viyudin@mail.ru*

Received August 28, 2024; revised August 28, 2024; accepted August 29, 2024

In this study, the Ramsey spectroscopy of coherent population trapping resonances excited on the D_1 line of alkali metal atoms in miniature vapor cells has been studied theoretically and experimentally. The configuration of the field produced by two counterpropagating waves with opposite circular polarizations has been considered. A counterpropagating wave is formed as a result of reflection from a partially transmitting output mirror, while the signal from the initial wave transmitted through the mirror is detected. It is shown that such a scheme is characterized by the optimal mirror reflection coefficient, for which the short-term stability can be substantially improved relative to the standard scheme without the counterpropagating wave. The three-fold improvement of the short-term stability of the atomic clock based on the coherent population trapping resonance in a vapor cell with ^{87}Rb atoms has been demonstrated experimentally.

DOI: 10.1134/S0021364024603130

1. INTRODUCTION

The atomic clock is a quantum instrument for high-precision measurements of frequency and time. The wide area of their application includes important fields such as navigation and positioning, data synchronization and transmission, metrology, geodesy, and verification of fundamental physical theories [1–9]. In miniature rf atomic clocks, coherent population trapping (CPT) resonances on the D_1 line of alkali metal atoms are widely used [10–14]. The advantages of such devices are their compactness and low energy consumption, which are ensured by the application of purely optical methods for exciting the resonance between hyperfine-structure components of the ground state.

One of the main problems limiting the long-term stability of atomic clocks is the light frequency shift of the reference transition during the interaction of atoms with a probe laser field. The devices based on the Ramsey spectroscopy of CPT resonances, for which various highly effective methods for suppressing the field shift can be used [10–24], possess a high potential for solving this problem [15–18].

However, apart from the long-term stability, the short-term stability that is affected by resonance parameters such as the amplitude and width is an important characteristic of atomic clocks. In the most widespread case of excitation of CPT resonances by circularly polarized light, optical pumping of atoms to the extreme Zeeman sublevel of the hyperfine component of the ground state with the maximum angular momentum takes place. The atoms accumulated in such a trapped state do not contribute to the formation of coherence between the working Zeeman sublevels with zero angular momentum projection. For this reason, the reference resonance amplitude does not reach its maximum possible value, which limits the short-term stability. To eliminate the trap state, a method for excitation of CPT resonances in the field formed by two counterpropagating waves with opposite circular polarizations (so-called $\sigma_+ - \sigma_-$ configurations) was developed in [25] and tested experimentally in [26] for continuous-wave spectroscopy. The variant of Ramsey spectroscopy in the $\sigma_+ - \sigma_-$ configuration was implemented only for laser-cooled atoms [27].

In this study, we investigate the possibility of significant improvement of the short-term stability of atomic clocks based on the Ramsey spectroscopy of CPT resonances in miniature vapor cells using the scheme proposed in [25]. In our case, the counterpropagating wave with the opposite circular polarization is produced using a partially transmitting mirror with

the possibility of varying the reflection coefficient. The calculations of the error signal for the D_1 line of ^{87}Rb atoms demonstrate the existence of the optimal reflection coefficient of the mirror, for which the slope of the discriminant curve is maximal. Theoretical conclusions are confirmed by the results of the experiment in which the short-term stability of the CPT clock was improved by a factor of 3 compared to the standard scheme without the counterpropagating wave.

2. THEORY

As a specific example, let us consider the interaction of the full hyperfine structure of the D_1 line of ^{87}Rb atoms with a sequence of Ramsey pulses of the bichromatic field produced by two counterpropagating resonant waves with opposite circular polarizations:

$$\mathbf{E}(t) = [E_1^{(+)}(t)e^{ik_1z}\mathbf{e}_{+1} + E_1^{(-)}(t)e^{-ik_1z}\mathbf{e}_{-1}]e^{-i[\omega_1 t+\varphi_1(t)]} + [E_2^{(+)}(t)e^{ik_2z}\mathbf{e}_{+1} + E_2^{(-)}(t)e^{-ik_2z}\mathbf{e}_{-1}]e^{-i[\omega_2 t+\varphi_2(t)]} + \text{c.c.}, \quad (1)$$

where $\mathbf{e}_{\pm1} = \pm(\mathbf{e}_x \pm i\mathbf{e}_y)/\sqrt{2}$ are the unit vectors of the right- (σ_+) and left-hand (σ_-) circular polarizations of light; $E_{1,2}^{(\pm)}(t)$ are the complex amplitudes of the corresponding spectral components; and the functions $\varphi_{1,2}(t)$ describe the field phase modulation used to generate the error signal. For definiteness, we assume that $\sigma_+ - \sigma_-$ is the configuration of the counterpropagating waves that is formed by the reflection of an incident bichromatic wave with the σ_+ polarization from a mirror and its transformation during the propagation through a $\lambda/4$ plate into the counterpropagating wave with the σ_- polarization as shown schematically in Fig. 1a. The energy level diagram for the D_1 line of ^{87}Rb and the diagram of light-induced transitions forming the CPT resonance between the states $|F_{g_1} = 2,\ m = 0\rangle$ and $|F_{g_2} = 1,\ m = 0\rangle$ are shown in Fig. 1b.

As demonstrated in [25], the CPT states for the D_1 line of alkali metal atoms for each of the counterpropagating σ_+ and σ_- waves (which are the superposition of the Zeeman sublevels $|F_{g_1}, m = 0\rangle$ and $|F_{g_2}, m = 0\rangle$ of the ground state) coincide provided that

$$2(k_1 - k_2)Z_{\text{mirr}} = (2n+1)\pi \quad (n = 0,1,2\ldots), \quad (2)$$

where Z_{mirr} is the distance to the mirror (see Fig. 1a). In this case, the constructive interference of two-photon transitions from different circular polarizations takes place, and the amplitude of the CPT resonance is maximal. However, for the fulfillment of condition (2) in an extended medium, miniature vapor cells must be used, the longitudinal size L of which should satisfy the condition

$$L \ll 2\pi/(k_1 - k_2). \quad (3)$$

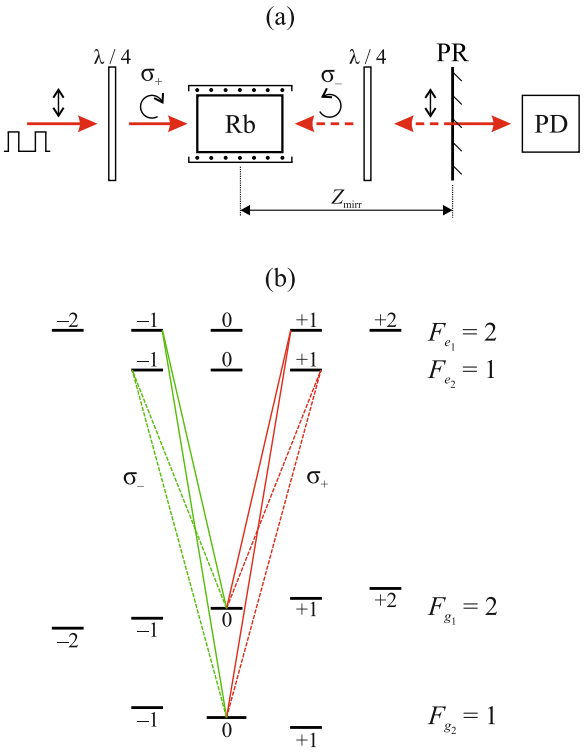

Fig. 1. (Color online) (a) Diagram of the formation of the $\sigma_+ - \sigma_-$ field configuration: (PR) partially transmitting mirror and (PD) photodetector. (b) Diagram of light-induced transitions involved in the excitation of the CPT resonance between the states $|F_{g_1} = 2,\ m = 0\rangle$ and $|F_{g_2} = 1,\ m = 0\rangle$ for the D_1 line of ^{87}Rb atoms in the $\sigma_+ - \sigma_-$ configuration of the bichromatic field.

In particular, for ^{87}Rb, vapor cells of length $L \ll 4.4$ cm must be used.

The temporal dynamics of atoms is described by the quantum kinetic equation for density matrix $\hat{\rho}$:

$$\frac{\partial}{\partial t}\hat{\rho}(t) + \hat{\Gamma}\{\hat{\rho}\} = -\frac{i}{\hbar}[(\hat{H}_0 + \hat{V}_E(t) + \hat{V}_B), \hat{\rho}], \quad (4)$$

where $\hat{H}_0$ is the Hamiltonian of an unperturbed atom; $\hat{V}_E(t) = -\hat{\mathbf{d}}\mathbf{E}(t)$ is the operator of the interaction of atoms with the laser field ($\hat{\mathbf{d}}$ is the electric dipole moment operator and $\mathbf{E}(t)$ is the electric field strength vector), and $\hat{V}_B = -\hat{\boldsymbol{\mu}}\mathbf{B}$ is the operator of the interaction of atoms with the static magnetic field, which is used to split the Zeeman sublevels ($\hat{\mu}$ is the magnetic moment operator and $\mathbf{B}$ is the magnetic induction vector); and $\hat{\Gamma}\{\hat{\rho}\}$ is the linear functional describing relaxation processes. The model includes the following relaxation constants: the rate of spontaneous decay of the excited state γ_{sp}; the decay rate of the optical coherence γ_{opt}, and the rates of relaxation of atoms γ_g and γ_e to the equilibrium isotropic distribution over

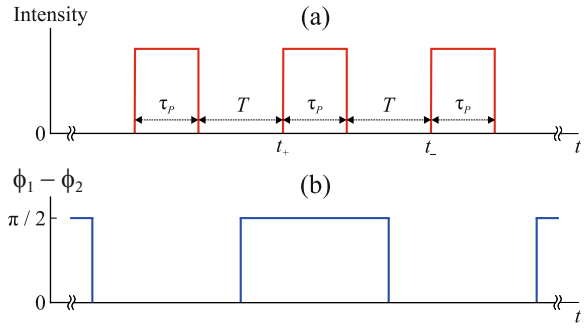

Fig. 2. (Color online) Schematic diagram of a periodic sequence of the Ramsey pulses with the duration τ_P and free evolution time T: (a) modulation of the field intensity and (b) modulation of the phase difference in the spectral components of the bichromatic field to form the error signal given by Eq. (6).

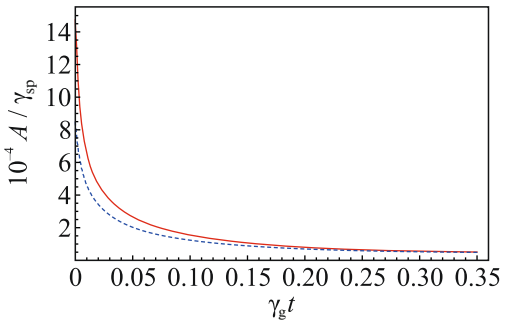

Fig. 3. (Color online) Temporal dynamics of the absorption signals (red solid line) $A^{(+)}(t,+\pi/2)$ and (blue dashed line) $A^{(+)}(t,-\pi/2)$ during the action of the Ramsey pulses according to the calculations with the parameters $R_1^{(+)}/\gamma_{sp} = R_2^{(+)}/\gamma_{sp} = 0.5$, $\alpha = 0.25$, $\tau_P = 0.5\gamma_g^{-1}$, $T = \gamma_g^{-1}$, $\Omega_L/\gamma_{sp} = 0.05$, $\gamma_{opt}/\gamma_{sp} = 50$, $\gamma_g/\gamma_{sp} = 10^{-5}$, $\gamma_e/\gamma_{sp} = 20$, and $\delta_R T = \pi/4$.

the Zeeman sublevels of the ground and excited states, respectively. We assume that the collisional broadening of the optical transition in the buffer gas exceeds the Doppler width (i.e., $\gamma_{opt} > k\bar{\upsilon}$, where $\bar{\upsilon}$ is the thermal velocity of atoms). In this case, we can disregard the Doppler effects associated with the motion of atoms and consider the model of motionless atoms.

In the approximation of an optically thin medium, the amplitude of the counterpropagating wave with the σ_- polarization is related to the amplitude of the incident wave with the σ_+ polarization as

$$|E_j^{(-)}|^2 = \alpha |E_j^{(+)}|^2, \quad 0 \le \alpha \le 1 \quad (j = 1,2), \qquad (5)$$

where α is a certain effective reflection coefficient determined by the sum of the reflection from the mirror and losses in optical elements of the setup. In our calculations, we used the Rabi frequencies $R_j^{(\pm)} = |d_{eg} E_j^{(\pm)}|/\hbar$ (where $d_{eg} = \langle J_e \| \hat{d} \| J_g \rangle$ is the reduced matrix element of the electric dipole moment operator) and the parameter $\Omega_L = \mu_B |\mathbf{B}|/\hbar$ characterizing the Zeeman splitting of hyperfine levels (where μ_B is the Bohr magneton).

As a spectroscopic signal, we consider the absorption of the incident wave with the σ_+ polarization. The frequency in the CPT clock is stabilized by the error signal for the Ramsey spectroscopy using the phase jump technique. In this case, the phase difference $\phi_1 - \phi_2$ of the frequency components for adjacent Ramsey pulses is $\pm\pi/2$. Figure 2 shows schematically a periodic sequence of Ramsey pulses and corresponding phase jumps. Here, each jump serves simultaneously for interrogation of atoms and their pumping to the CPT state. The error signal is formed as the difference in the integral absorption signals between adjacent Ramsey pulses, which can be represented analytically by the following relation:

$$S(\delta_R) = \int_{t_+}^{\tau_P} A^{(+)}(t,+\pi/2)dt - \int_{t_-}^{\tau_P} A^{(+)}(t,-\pi/2)dt, \qquad (6)$$

where $A^{(+)}(t,\pm\pi/2)$ is the signal of the absorption of the wave with the right-hand circular polarization (σ_+) for the phase difference $\phi_1 - \phi_2 = \pm\pi/2$ of the frequency components and $\delta_R = (\omega_1 - \omega_2 - \omega_{hfs})$ is the Raman detuning (where ω_{hfs} is the hyperfine splitting frequency of the ground state). For illustration, Fig. 3 shows the results of calculation of the temporal dynamics of signals $A^{(+)}(t,\pm\pi/2)$ during the action of Ramsey pulses.

As seen in Fig. 4, the advantage of the $\sigma_+ - \sigma_-$ configuration as compared with the conventional scheme (i.e., a single circularly polarized traveling wave) is the significant increase in the error signal amplitude. This occurs because the counterpropagating wave with the σ_- polarization pumps out atoms from the extreme Zeeman sublevel $|F_{g_1} = 2,\ m = 2\rangle$, which does not interact with the σ_+ field, thus increasing the number of atoms in the CPT state. In addition, the resonance width is independent of the field intensity (in contrast to continuous wave spectroscopy) and is determined only by the free evolution time.

One of the key parameters affecting the short-term stability is the slope of the linear part of the error signal at the center of the resonance:

$$K = \left.\frac{\partial S}{\partial \delta_R}\right|_{\delta_R = 0}. \qquad (7)$$

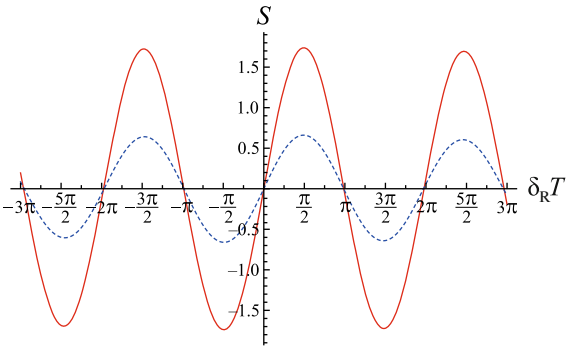

Fig. 4. (Color online) Error signal $S(\delta_R)$ versus the two-photon detuning at the reflection coefficients $\alpha = 0.25$ (red solid line) and $\alpha = 0$ (blue dashed line, which corresponds to the standard scheme without a counterpropagating wave) according to the calculations with the parameters $R_1^{(+)}/\gamma_{sp} = R_2^{(+)}/\gamma_{sp} = 0.5$, $\tau_P = 0.5\gamma_g^{-1}$, $T = \gamma_g^{-1}$, $\Omega_L/\gamma_{sp} = 0.05$, $\gamma_{opt}/\gamma_{sp} = 50$, $\gamma_g/\gamma_{sp} = 10^{-5}$, and $\gamma_e/\gamma_{sp} = 20$.

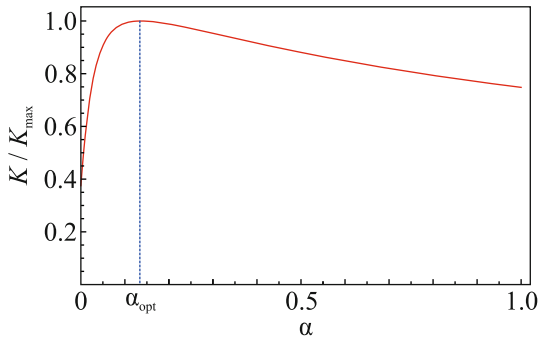

Fig. 5. (Color online) Slope of the error signal K at the line center versus the reflection coefficient α according to the calculations with the parameters $R_1^{(+)}/\gamma_{sp} = R_2^{(+)}/\gamma_{sp} = 0.5$, $\tau_P = \gamma_g^{-1}$, $T = \gamma_g^{-1}$, $\Omega_L/\gamma_{sp} = 0.05$, $\gamma_{opt}/\gamma_{sp} = 50$, $\gamma_g/\gamma_{sp} = 10^{-5}$, and $\gamma_e/\gamma_{sp} = 20$.

Figure 5 shows the dependence of the slope K on the reflection coefficient α, which specifies the relation between the amplitudes of the incident and counterpropagating waves. It can be seen that the existence of the counterpropagating wave with the opposite circular polarization ($\alpha > 0$) leads to an increase in the slope of the error signal as compared to the scheme without the reflected wave ($\alpha = 0$). In this case, the dependence $K(\alpha)$ has a clearly manifested maximum. The existence of the optimal reflection coefficient is physically explained by the existence of two competing processes in the given spectroscopic scheme, for which balance is achieved at a certain reflection coefficient $\alpha = \alpha_{opt}$. On the one hand, an increase in the reflection coefficient of the mirror leads to an increase in the amplitude of the counterpropagating wave with the σ_- polarization and, hence, increases the rate of pumping of atoms from the trapped state. As a result, the fraction of atoms in the CPT state increases, which leads to an increase in the resonance amplitude. On the other hand, the atoms absorbing the reflected wave make no contribution to the absorption of the detected σ_+ wave, thus reducing the resonance amplitude. Therefore, with increasing α, the resonance amplitude for the detected wave first increases due to the pumping of atoms from the trapped state $|F_{g_1} = 2, m = 2\rangle$ to the CPT state, and then begins to decrease because of the increase in the fraction of atoms involved in the absorption of the counterpropagating wave. For a certain relation between the intensities of the counterpropagating waves, which corresponds to the optimal reflection coefficient α_{opt}, the peak in the slope of the error signal given by Eq. (6) is observed. The position of this peak depends on the intensity of the incident wave and on the relaxation constants that determine the processes of optical pumping of atoms.

3. EXPERIMENT

The diagram of the experimental setup is shown in Fig. 6. As the radiation source, we used a distributed Bragg reflector laser with a fiber output and a wavelength of 795 nm, which corresponds to the D_1 absorption line of ^{87}Rb atoms. The vapor cell had the internal longitudinal dimension $L = 5$ mm, which satisfied criterion (3). Phase modulation of radiation at half the frequency of the hyperfine splitting of the ground state was performed using the fiber electro-optic phase modulator. The half-wave plate together with the polarization splitter was used to control the power of radiation incident on the cell. The experimental setup also included three quarter-wave plates. The first plate formed the circular σ_+ polarization of the incident wave, while the second plate formed the opposite σ_- polarization of the counterpropagating wave. The third plate together with the polarization splitter and the totally reflecting mirror formed the effective output mirror with a variable reflection coefficient. In this case, the reflection coefficient was varied by rotating the quarter-wave plate. Depending on the rotational angle of this plate, the relation between the radiation reaching the photodetector and the radiation with the σ_- polarization, which was reflected back to the vapor cell, changed. All optical elements had an antireflection coating; when the position of the wave plate corresponded to the minimum reflection coefficient of the output mirror, at least 98% of light with the σ_+ polarization transmitted through the cell reached the photodetector. In our experiments, we used the Ramsey sequence of pulses with a duration of 600 μs and a free evolution time of 400 μs.

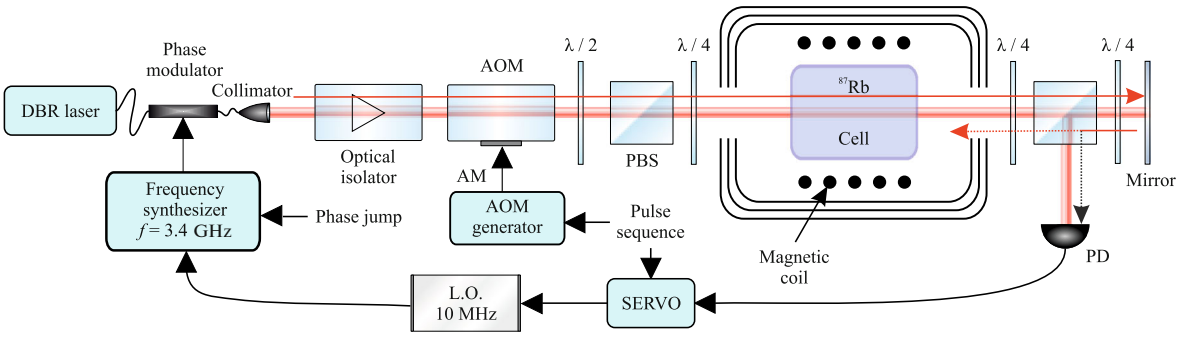

Fig. 6. (Color online) Schematic diagram of the experimental setup: (AOM) acousto-optic modulator, (L.O.) local quartz oscillator, (λ/2) half-wave plate, (λ/4) quarter-wave plate, (PD) photodetector, (PBS) polarization band splitter, (AOM generator) generator of the signal fed to AOM, (AM) amplitude modulation signal. To measure the reflected wave power, the quarter-wave plate located between the PBS and the mirror was rotated.

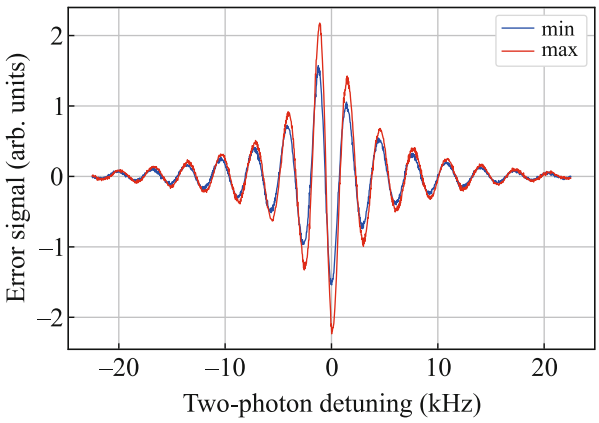

Fig. 7. (Color online) Ramsey structures in the error signal in different positions of the totally reflecting mirror relative to the cell corresponding to (blue line) the destructive interference of two-photon transitions for the σ_+ and σ_- counterpropagating waves and (red line) the constructive interference, for which condition (2) holds.

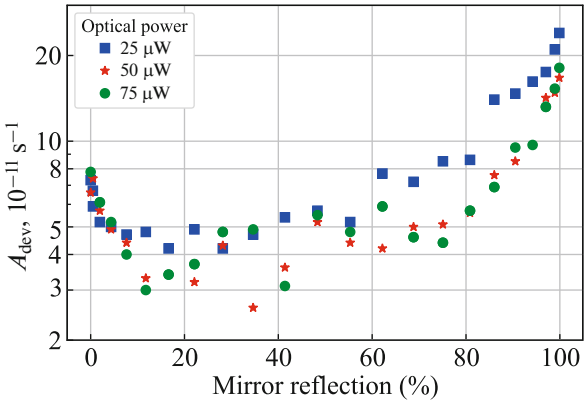

Fig. 8. (Color online) Short-term stability versus the reflection coefficient of the effective output mirror for different radiation powers. Zero reflection coefficient corresponds to the absence of the reflected wave.

Since the error signal amplitude depends periodically on the distance between the totally reflecting mirror and the cell, at the first stage, we optimized the position of the cell relative to this mirror to satisfy condition (2). Figure 7 shows two error signals for different positions of the cell, in which the maximum and minimum amplitudes of the CPT resonance are reached. It is seen that the difference between these amplitudes is about 30% and is due to the constructive and destructive interferences of two-photon transitions for the incident and counterpropagating waves [25].

Further, for the optimal position of the totally reflecting mirror, we measured the dependence of the short-term stability frequency on the reflection coefficient of the effective output mirror for different radiation powers. Figure 8 shows that these dependences are identical in character: upon an increase in the reflection coefficient to 30–40%, the stability is improved, but then becomes worsened; in other words, there is the optimal reflection coefficient α_{opt} of the mirror. In particular, for a radiation power of 50 μW, the stability was improved from 7.6×10^{-11} to 2.6×10^{-11} (i.e., by a factor of 3) during 1 s. These results are in good qualitative agreement with the theoretical conclusions drawn above.

4. CONCLUSIONS

For miniature vapor cells, we have investigated the Ramsey spectroscopy of CPT resonances excited by a laser field with the $\sigma_+ - \sigma_-$ configuration formed by two counterpropagating waves with opposite circular polarizations. In our scheme, a counterpropagating wave is formed by a partially transmitting mirror, while the spectroscopic signal is detected in the transmitted wave. It has been shown theoretically and experimentally that there is an optimal reflection coefficient of the output mirror corresponding to the best short-term stability. In our setup, the short-term stability has

been improved by three times (from 7.6×10^{-11} to 2.6×10^{-11} in 1 s) as compared to the standard scheme without the counterpropagating wave. The results of this study can be generalized to the D_1 line of atoms of other alkali metals (e.g., ^{85}Rb and ^{133}Cs).

FUNDING

This study was supported by the Russian Science Foundation (project no. 22-72-10096). V.I. Yudin and S.M. Kobtsev acknowledge the support of the Ministry of Science and Higher Education of the Russian Federation (project no. FSUS-2020-0036).

CONFLICT OF INTEREST

The authors of this work declare that they have no conflict of interests.

REFERENCES

1. L. Maleki and J. Prestage, Metrologia **42**, S145 (2005).
2. M. S. Grewal, L. R. Weill, and A. P. Andrews, *Global Positioning Systems, Inertial Navigation, and Integration* (Wiley-Interscience, Hoboken, NJ, 2007).
3. J. D. Prestage and G. L. Weaver, Proc. IEEE **95**, 2235 (2007).
4. A. Derevianko and M. Pospelov, Nat. Phys. **10**, 933 (2014).
5. Y. Bock and D. Melgar, Rep. Prog. Phys. **79**, 106801 (2016).
6. C. Lisdat, G. Grosche, N. Quintin, et al., Nat. Commun. **7**, 12443 (2016).
7. M. Kajita, *Measuring Time: Frequency Measurements and Related Developments in Physics* (IOP Publ., Bristol, UK, 2018).
8. T. E. Mehlstäubler, G. Grosche, Chr. Lisdat, P. O. Schmidt, and H. Denker, Rep. Prog. Phys. **81**, 064401 (2018).
9. T. N. Bandi, BEMS Rep. **9**, 1 (2023).
10. J. Vanier, Appl. Phys. B **81**, 421 (2005).
11. V. Shah and J. Kitching, Adv. At. Mol. Opt. Phys. **59**, 21 (2010).
12. S. Knappe, P. D. D. Schwindt, V. Shah, L. Hollberg, J. Kitching, L. Liew, and J. Moreland, Opt. Express **13**, 1249 (2005).
13. Z. Wang, Chin. Phys. B **23**, 030601 (2014).
14. J. Kitching, Appl. Phys. Rev. **5**, 031302 (2018).
15. T. Zanon, S. Guerandel, E. de Clercq, D. Holleville, N. Dimarcq, and A. Clairon, Phys. Rev. Lett. **94**, 193002 (2005).
16. C. M. Rivera-Aguilar, M. Callejo, A. Mursa, C. Carlé, R. Vicarini, M. Abdel Hafiz, J.-M. Friedt, N. Passilly, and R. Boudot, Appl. Phys. Lett. **124**, 114102 (2024).
17. G. V. Voloshin, K. A. Barantsev, and A. N. Litvinov, J. Exp. Theor. Phys. **138** (3) (2024, in press).
18. D. S. Chuchelov, M. I. Vas'kovskaya, E. A. Tsygankov, S. A. Zibrov, K. M. Sabakar, V. V. Vassiliev, and V. L. Velichansky, JETP Lett. **119**, 16 (2024).
19. V. I. Yudin, A. V. Taichenachev, M. Yu. Basalaev, T. Zanon-Willette, J. W. Pollock, M. Shuker, E. A. Donley, and J. Kitching, Phys. Rev. Appl. **9**, 054034 (2018).
20. V. I. Yudin, A. V. Taichenachev, M. Yu. Basalaev, T. E. Mehlstäubler, R. Boudot, T. Zanon-Willette, J. W. Pollock, M. Shuker, E. A. Donley, and J. Kitching, New J. Phys. **20**, 123016 (2018).
21. M. Abdel Hafiz, G. Coget, M. Petersen, C. Rocher, S. Guerandel, T. Zanon-Willette, E. de Clercq, and R. Boudot, Phys. Rev. Appl. **9**, 064002 (2018).
22. M. Shuker, J. W. Pollock, R. Boudot, V. I. Yudin, A. V. Taichenachev, J. Kitching, and E. A. Donley, Phys. Rev. Lett. **122**, 113601 (2019).
23. M. Shuker, J. W. Pollock, R. Boudot, V. I. Yudin, A. V. Taichenachev, J. Kitching, and E. A. Donley, Appl. Phys. Lett. **114**, 141106 (2019).
24. M. Yu. Basalaev, V. I. Yudin, D. V. Kovalenko, T. Zanon-Willette, and A. V. Taichenachev, Phys. Rev. A **102**, 013511 (2020).
25. A. V. Taichenachev, V. I. Yudin, V. L. Velichansky, S. V. Kargapoltsev, R. Wynands, J. Kitching, and L. Hollberg, JETP Lett. **80**, 236 (2004).
26. S. V. Kargapoltsev, J. Kitching, L. Hollberg, A. V. Taichenachev, V. L. Velichansky, and V. I. Yudin, Laser Phys. Lett. **1**, 495 (2004).
27. X. Liu, V. I. Yudin, A. V. Taichenachev, J. Kitching, and E. A. Donley, Appl. Phys. Lett. **111**, 224102 (2017).

Translated by N. Wadhwa